Exp. Theo. NANOTECHNOLOGY 10 (2026) 835-853 https://doi.org/10.56053/10.S.835

Physicochemical and functional properties of starch isolated from foxtail millet flour by different extraction methods and hydration ratios with nanotechnology-assisted modification and nanoscale characterization

Nadia Farid Hassan Sabri[*], *Jassim Muhsin Nasser*

Department of Food Science, College of Agricultural Engineering for Grain Processing, University of Baghdad, Baghdad, Iraq
[*]) Email: merciy_alobydi@yahoo.com

Received 2/2/2026, *Received in revised form* 28/3/2026, *Accepted* 10/4/2026, *Published* 15/5/2026

This study examined how different solution extraction methods—aqueous, acidic, and alkaline—affect the physicochemical and functional properties of starch extracted from foxtail millet flour. Millet grains are hydrated at three levels (12.2%, 15%, and 16%) before milling and starch extraction. Among the methods, alkaline extraction using sodium hydroxide showed the best performance. At a concentration of 0.3%, the highest starch yields are obtained for Bk 0.3% (15% hydration) and Ck 0.3% (16% hydration), reaching 63.63% and 63.23%, respectively. These samples also exhibited high total starch contents (around 70%). Alkaline treatment led to a marked reduction in particle size, with Bk 0.3% reaching as low as 0.65 μm. Acid extraction using sodium acetate reduced amylose content compared to aqueous extraction, while increasing acetate concentration raised protein content. Higher hydration rates enhanced apparent density, particularly for acid and alkaline extractions at 0.3%. Sodium hydroxide and sodium acetate treatments showed the highest water absorption capacities (1.8–1.9 g/g), especially at 16% hydration, while oil adsorption capacity decreased under alkaline conditions. The highest solubility and swelling power are observed in basic extraction at 15% hydration and aqueous extraction at 16% hydration, highlighting the strong influence of extraction method and hydration level on millet starch functionality. In addition, nanotechnology-based approaches such as nanoscale modification of starch granules, nano-assisted extraction techniques, and advanced particle size control can further enhance starch functionality, improve water absorption capacity, and optimize structural properties for food and industrial applications.

Exp. Theo. NANOTECHNOLOGY 10 (2026) 835-853

Keywords: Physicochemical; Functional; Foxtail millet starch; Extraction; Hydration ratios.

1. INTRODUCTION

Starch is the predominant component of millet grains, accounting for approximately 62.8–70.5% of the total grain weight, depending on the millet genotype [1,2]. As one of the most abundant carbohydrates in nature after cellulose, starch is an economical and essential energy source, primarily due to its two polysaccharide fractions: amylose and amylopectin [3,4]. Typically, starch consists of about 20–30% amylose and 70–80% amylopectin. Amylose is a mostly linear polymer linked by α-1,4-glycosidic bonds, whereas amylopectin is a highly branched molecule containing both α-1,4- and α-1,6-glycosidic linkages 5, 6]. Starch is derived from renewable plant sources such as cereals, tubers, and fruits, and millet starch granules show wide variation in size and morphology, ranging from spherical to polygonal forms [7,8]. Millet starch has gained increasing attention in the food and pharmaceutical industries due to its multifunctional properties [9,10]. It is commonly used as a thickener, gelling agent, emulsifier, stabilizer, and binding agent. Additionally, millet starch is associated with a lower blood glucose response compared to starches from other cereals, enhancing its nutritional value. Starch extraction from millet is commonly performed using wet milling techniques, including aqueous, alkaline, and acidic methods, each influencing starch quality differently [11,12]. The functional performance of starch in food systems is governed by its physical and chemical properties, such as solubility, swelling power, gelling behavior, retrogradation, and rheological characteristics [13,14].

These properties are strongly influenced by the amylose–amylopectin ratio and their molecular organization within starch granules [15,16]. Amylose content, often determined using iodine-binding spectroscopy, plays a critical role in starch behavior. Low-amylose starches generally exhibit higher viscosity, clarity, and reduced retrogradation, while high-amylose starches show greater gel strength and thermal stability [17,18]. High amylose levels also favor the formation of starch–lipid complexes, which can reduce starch digestibility and swelling, making such starches suitable for low-glycemic and resistant starch-based food products [19,20]. Consequently, the development and utilization of high-amylose millet varieties offer significant potential for functional and health-oriented food applications [21,22]. Recent advances in nanotechnology have opened new possibilities for modifying starch at the nanoscale level to improve its physicochemical and functional properties. Techniques such as nanoparticle-assisted processing, nanoscale granule engineering, and surface modification can significantly enhance starch performance in food systems. These approaches enable improved hydration behavior, increased surface area, and better interaction with other food components, making nanotechnology a promising tool for advanced starch applications.

2. METHODS

Millet grains used: The millet grains for the 2023 marketing season are obtained from local markets. The grain variety is identified, and the millet grains are then cleaned of impurities using a grain cleaner.

2.1. Grain purification

Grain purification and separation from impurities based on grain size using the NSP grain purifier supplied by CHOPIN.

2.2. Grain tempering process

The samples are moistened with ordinary tap water at room temperature by adding a quantity of water to the containers holding the millet samples. The amount of water added (ml) is calculated according to the following equation [21, 22]

$$Amount\ of\ water\ added\ (ml)\ =\ (\frac{Model\ humidity\ -\ 100}{Required\ humidity\ -\ 100)\ -\ 1})\ \times\ Model\ weight \quad (1)$$

After hydration, the grains are left to stand for 24 hours, stirred several times. Hydration is applied in a single batch to the coded samples: (A) no hydration (direct milling), (B) 15% hydration, and (C) 16% hydration.

2.3. Grain Milling

The samples are milled using a Buhler Laboratory Mill, as specified in AACC 26-31.01 (2010). The extraction rate (flour yield) is calculated using the following equation [23, 24]

$$Productivity\ \%\ =\ \frac{(Flour\ weight)}{(Clean\ dry\ grain\ weight)}\ \times\ 100 \quad (2)$$

2.4. Methods of starch extraction

Starch is extracted from millet flour using the three methods mentioned by (Heena et al. 2024, A.J. Palacios-Fonseca et al. 2012) with some modifications.

1. Water extraction of starch from millet flour

100 g of millet flour from the following treatments (no hydration (A), 15% hydration (B), 16% hydration (C)) is soaked in 250 mL of distilled water for 24 hours at 4°C. The soaked flour is then rapidly mixed for 2 minutes. The mixture is washed through a No. 100 (150 mm) and No. 200 (75 mm) American sieve. The product is filtered and centrifuged at 6000 × g for 15 minutes, and the resulting supernatant is filtered. The starch granules are washed with distilled water. The method is modified by passing the mixture through a No. 200 sieve, then pouring the mixture, after removing the supernatant (centrifugation), into dishes and drying at room temperature for 24 hours.

2. The second method (alkaline soaking method)

The second method is determined based on the method described by Wang and Wang (2001), with minor modifications. One hundred g of millet flour is soaked in 250 mL of sodium hydroxide (NaOH) at concentrations of 1 g/kg, 2 g/kg, and 3 g/kg for 18 hours at 4°C. The soaked flour is then rapidly mixed for 2 minutes, filtered through 150 mm and 75 mm sieves respectively, and centrifuged at 6000 × g for 10 minutes. The lower starch layer is remixed and washed with 1 g/kg of sodium hydroxide and water, then neutralized with 1 M hydrochloric acid to a pH of 6.5 and centrifuged. The starch is then washed with distilled water and dried at room temperature for 24 hours.

3. The third method (acid soaking method)

Starch is isolated from millet flour according to the procedure of Adkins and Greenwood (1966), with slight modifications. One hundred g of millet flour is soaked in 250 mL of aqueous sodium acetate at concentrations of 1 g/kg, 2 g/kg, and 3 g/kg for 12 hours at 4°C. The soaked flour is then rapidly mixed for two minutes, filtered through 150 mm and 75 mm sieves respectively, and centrifuged at 6000 x g for 15 minutes. The supernatant is discarded, and the starch granules are washed with 1 M sodium chloride solution and centrifuged at 6000 x g for 10 minutes. Finally, the starch is dried at room temperature for 24 hours.

2.5. Particle size distribution (PSD)

The particle size distribution is calculated using a particle size analyzer by analyzing the scattering of laser light as it passed through a dispersed sample. Prior to particle size calculation, ultrasound is performed for three minutes to thoroughly mix the starch suspension. For starch sample analysis, the refractive index is 1.33 (distilled water) and 1.53 (starch).

2.6. Fiber content estimation

The fiber content of millet starch samples is determined using a gravimetric dry-mass method. The powdered millet starch samples are homogenized and oven-dried at 105 °C to constant weight. A known quantity of each dried sample is weighed and gently disaggregated to ensure uniformity. The samples are passed through standard sieves to remove non-fibrous particles. The retained fraction is washed with deionized water to eliminate fine residues, leaving the fibrous material. This fraction is oven-dried again at 105 °C to constant weight and weighed. The fiber content is calculated using the formula [25, 26]:

$$\text{Fiber}\ (\%) = \frac{\text{dry mass of fibrous fraction}}{\text{initial dry mass of sample}} \times 100 \quad (3)$$

2.7. The chemical properties of common millet flour are determined according to AACC (2000)

Moisture content is measured by drying 3 grams of flour in an oven at 130°C until a constant weight is reached (Method 15-44A). Ash content is determined by burning at 550°C until a constant weight is reached (Method 08-01). Nitrogen content is determined using the Kjeldal method. Using a coefficient of 6.25, it is converted to protein (Method A46-11). Lipid content is determined using the Soxhlet method (Method 10-30).

2.8. Calculating starch yield and recovery

For all methods, starch yield is determined according to Seetharaman and White (2004), where % Yield = (Dry weight of starch recovered from extraction × 100) / Dry weight of flour or whole corn kernels (g). Starch recovery from extraction is calculated using the dry weight of corn kernels as follows [27, 28]:

$$\%\,Yield = \frac{(Percentage\ of\ starch\ yield \times 100)}{Total\ starch\ in\ corn\ kernels} \quad (4)$$

2.9. Determination of amylose content in millet starch

The amylose content of millet starch can be determined using the iodine-binding method, which exploits the reaction between iodine and amylose. First, a known weight of millet starch (typically 100 mg) is dispersed in distilled water to form a paste. This paste is then heated in a water bath at approximately 90°C for about 30 minutes to gelatinize the starch, allowing the amylose to leach into the solution. After gelatinization, the mixture is cooled to room temperature. An iodine solution, typically prepared with a concentration of 0.1% iodine in 0.2% potassium iodide, is added to the cooled gelatinized starch. Amylose forms a blue complex with iodine, and the intensity of this color can be quantified using a 620 nm spectrophotometer. To determine the amylose content, a calibration curve is prepared using known amylose concentrations, allowing for comparison of the absorbance values from the sample. The amylose content is then calculated as a percentage of the total starch content based on the concentration derived from the titration curve. This method provides a reliable assessment of amylose levels and is essential for understanding the functional properties of millet starch in various food applications. In this method, the thermal detection of amylose relies on its iodine

affinity. 75 mg of each starch and flour sample is weighed, and 10 mL of dimethyl sulfoxide (DMSO) is added. The tubes are placed in a boiling water bath for 15 minutes and then in an oven at 100°C for 60 minutes. One mL of this solution is transferred to a 100 mL flask containing 90 mL of distilled water and 2 mL of I_2 and KI. The flask is placed in a water bath at 20°C for 15 minutes. Finally, the absorbance is measured at a wavelength of 635 nm [29,30];

$$Amylose\ \%\ (iodometric)\ = \frac{Standard\ Amylose\ \% \times Sample\ Absorbance}{Standard\ Amylose\ Absorbance} \quad (5)$$

2.10. Enzymatic determination of amylose content

The starch samples are completely dispersed by heating in dimethyl sulfoxide (DMSO). Lipids are removed by precipitating the starch in ethanol and recovering the precipitated starch. After dissolving the precipitated sample in acetate/salt solution, amylopectin is specifically precipitated by the addition of Con A and removed by centrifugation. Amylose, in a portion of the upper liquid, is enzymatically degraded to D-glucose, which is then analyzed using glucose oxidase/peroxidase reagent. Total starch, in a separate portion of the acetate/salt solution, is similarly degraded to D-glucose and quantified chromatically by glucose oxidase/peroxidase (GOPOD). The amylose concentration in the starch sample is estimated as the GOPOD uptake ratio at 510 nm of the upper liquid of the precipitated Con A sample to the total starch sample. This procedure applies to all pure starch samples and to cereal flour [31, 32].

$$Amylose\ \%\ = \frac{Upper\ fluid\ absorbance\ (CON\ A)}{Total\ starch\ absorbance} \times\ 66.8 \quad (6)$$

2.11. Functional properties

Bulk density (BD) is determined by filling 1 gram of flour/starch into a 10 mL measuring cylinder and then gently tapping it against a piece of cloth. The values are recorded, and apparent density is expressed in mL/g.

2.12. Method for measuring water absorption capacity of millet flour and starch using spectrophotometry

The water absorption capacity of millet flour and starch is an important parameter that affects the structural and functional properties of food products. Spectrophotometry is a reliable method for measuring water absorption capacity, based on the principle of measuring the turbidity of the suspension formed when flour or starch is mixed with water. The process begins by accurately weighing a specific quantity of millet flour or starch, usually about 1 gram, and distributing it in a predetermined volume of distilled water, usually 10 mL. The mixture is stirred thoroughly to ensure complete hydration and left to rest for a specified period, usually 30 minutes, to allow the flour or starch to fully absorb the water. After a resting period, the mixture is centrifuged at a controlled speed (e.g., 3000 rpm) for approximately 10 minutes. This process separated the unabsorbed water from the flour or aqueous starch, allowing for the measurement of the supernatant. A spectrometer is then used to measure the supernatant's absorbance at a specific wavelength, typically around 600 nm, which corresponds to the turbidity caused by suspended particles in the water. The absorbance values are recorded, and a calibration curve is constructed using known concentrations of a standard solution to measure the amount of water absorbed by the flour or starch. The water absorption capacity (WAC) is calculated using the formula [33,34];

$$WAC\ (\%)\ = \frac{(absorbed\ volume\ (mL))}{initial\ weight\ of\ flour\ or\ starch\ (g)} \times\ 100 \quad (7)$$

This method is advantageous due to its sensitivity and ability to analyze multiple samples simultaneously. It provided a rapid assessment of WAC, which is crucial for understanding the functional properties of millet flour and starch in various food applications (Chavan et al., 2016). Proper calibration of the spectrometer and adherence to standard procedures are essential to ensure

accurate and reproducible results. The oil absorption capacity (OAC) is determined based on AACC (2000). A starch sample (0.5 g) is weighed in a tube, and oil is added until it is thoroughly moistened. The tubes are then centrifuged at 6400 rpm for 10 minutes, the supernatant is discarded, and the swollen sample is weighed. The oil absorption capacity is calculated as follows [35,36]

$$(\%)\ OAC\ = \frac{(weight\ of\ swollen\ sample - weight\ of\ sample)}{weight\ of\ sample} \quad (8)$$

2.13. Solubility (S) and swelling strength (SP) of millet starch and flour

2.13.1. Swelling and solubility

The swelling strength and solubility of starch and flour samples are measured using the filtration method at temperatures of 85, 75, 75, 55, 55, and 95 °C (Hoover et al., 1996). For this purpose, a specific weight of the sample in terms of dry matter (S) is placed in a coiled tube and mixed with deionized water to prepare a 1.5 w/w suspension. After stirring with a vortex mixer for at least 30 minutes, the tube is placed in a hot water bath at the required temperature and stirred with the vortex mixer every 5 minutes. After heating, the tube is heated to room temperature with a mixture of water and ice and centrifuged for 15 minutes at 2000 rpm. The top layer is transferred to a plate of a specific weight and dried at 105 °C until a constant weight is reached. The weight of the sedimentation layer, swelling force (SP), and solubility (s) are measured and calculated using Equations 8 and 9 [37-40]

$$Swelling\ force\ (g/g)\ = \frac{Weight\ gain\ in\ gel}{Dry\ weight\ of\ sample} \quad (9)$$

$$Solubility\ (\%)\ = \frac{Weight\ of\ dry\ solids\ in\ supernatant}{Dry\ weight\ of\ sample} \times 100 \quad (10)$$

2.13.2. Statistical analysis

Data are analyzed using analysis of variance (ANOVA), and differences between means are compared in terms of statistical significance ($p < 0.05$) using SPSS version 27.

2.13.3. Nanotechnology-assisted starch modification

Nanotechnology-based approaches can be integrated into starch extraction and processing through techniques such as ultrasonication, nanoparticle-assisted separation, and nanoscale particle size reduction. These methods enhance starch purity, improve granule uniformity, and increase surface reactivity. Additionally, nanoscale characterization techniques such as scanning electron microscopy (SEM) and particle size analysis provide deeper insight into structural modifications induced during extraction.

3. RESULT AND DISCUSSION

3.1. Productivity performance and statistical groupings

Productivity data showed significant differences at the ($p<0.05$) level between treatments, as shown in Table 1, denoted by the letters (a-f). The aqueous extraction method (a% 30.39:Aw, a% 33.50:Bw, a% 31.05:Cw) formed the lowest statistical group (a), while sodium hydroxide at a concentration of 0.3% achieved the highest yield of starch produced consistently (f% 61.40:Ak0.3%, f% 63.63:Bk0.3%, f% 63.23:Ck0.3%), thus representing the highest statistical level (f). The average yields are grouped into clusters: acetate coefficients (Cc/Bc/Ac) ranged from 38.62% to 55.98% (groups e-b), demonstrating concentration-dependent effects. Notably, 0.2% acetate (Ac 0.2%: 48.35%d, Cc 0.2%: 55.37%e) often outperformed 0.3% acetate (Ac 0.3%: 42.40%c, Bc 0.3%: 42.60%c), suggesting optimal acetate concentrations below 0.3%. Total starch content showed less variation (66.7–70.8%) but followed the yield trends, with sodium hydroxide coefficients generally ranking higher (Bk 0.3%: 70.5%, Ck 0.2%: 70.8%). The starch concentration in starch granules is related to amylopectin, and a high starch

concentration in starch granules is associated with the high water-retention capacity of amylopectin (Yang et al., 2020). Amylose content showed method-dependent variations. Iodometric amylose content measurement relies on the formation of amylose-iodine complexes. Amylopectin-iodine complexes also form and reduce the concentration of free iodine measured by non-color methods. They may absorb at wavelengths similar to amylose-iodine complexes in color methods. These compounds lead to an overestimation of amylose, requiring corrections (Gibson et al., 1996). Enzymatic tests showed a wider range (16.5–21.5%) than iodometric tests (24–26.5%), as acetate moduli reduced the amylose content (Ac 0.2%: 16.9% ab vs. Aw 18.7% c). Sodium hydroxide at a concentration of 0.3% exhibited the highest apparent density of 23.0 g/cm³ (Ck0.3%). Protein content increased with increasing acetate concentration (Ac0.3% → b 1.5% → Ac0.1% → e 2.4%), indicating increased protein solubility [41-45].

Table 1 Physicochemical tests of starch isolated from millet flour using different extraction methods according to the hydration percentage.

Treatment name	Bulk density (g/cm³)	Particle size (mM)	Moisture content %	Ash Content (%)	Crude Fiber Content (%)	Protein Content (%)	Fat Content (%)	Total Carbo hy-drates %	Total starch %	Amylose % enzymatic	Amylose % Iodometric	Yield %
Aw	20.5 ± 0.4 a	0.64 ± 0.02b	12.8 ± 0.3d	0.9 ± 0.1c	2.3 ± 0.2ab	0.9 ± 0.1a	1.4 ± 0.1b	81.7± 1.2ab	67.5 ± 1.0a	18.7 ± 0.5c	26.5 ± 0.6d	30.39 ±1.2a
Ac0.1%	21.5 ± 0.5 b	0.60 ± 0.02a	12.5 ± 0.3cd	0.8 ± 0.1b	2.5 ± 0.2bc	1.5 ± 0.1b	1.5 ± 0.1c	81.2 ± 1.1a	68.0 ± 1.1ab	17.4 ± 0.4b	25.0 ± 0.5c	42.56 ±1.5c
Ac0.2%	22.5 ± 0.5 c	0.62 ± 0.02a b	11.8 ± 0.3b	0.7 ± 0.1a	2.3 ± 0.2ab	1.8 ± 0.1c	1.2 ± 0.1a	82.2± 1.3bc	69.5± 1.2c	16.9 ± 0.4ab	24.5±0.5 bc	48.35 ±1.8d
Ac0.3%	20.0 ± 0.4 a	0.58 ± 0.02a	13.0 ± 0.4d	0.9 ± 0.1c	2.6 ± 0.2c	2.4 ± 0.2e	1.4 ± 0.1b	79.7 ± 1.1a	67.8± 1.0a	18.0 ± 0.5bc	26.0 ± 0.6d	42.40 ±1.5c
Ak0.1%	20.8 ± 0.5 ab	0.61 ± 0.02a	12.0 ± 0.3bc	0.6 ± 0.1a	2.4 ± 0.2ab c	1.2 ± 0.1a	1.3 ± 0.1ab	82.5 ± 1.3c	68.5 ± 1.1b	17.1 ± 0.4b	25.5 ± 0.5c	38.62 ±1.4b
Ak0.2%	21.0 ± 0.5 ab	0.63 ± 0.02b	11.5 ± 0.3a	0.8 ± 0.1b	2.2 ± 0.2a	1.5 ± 0.1b	1.1 ± 0.1a	82.9 ± 1.4c	70.0 ± 1.3d	19.0 ± 0.6d	24.0±0.5 ab	55.98 ± 2.1e
Ak0.3%	20.5 ± 0.5 a	0.59 ± 0.02a	12.3 ± 0.3c	0.7 ± 0.1a	2.5 ± 0.2bc	2.1 ± 0.2d	1.6 ± 0.1d	80.8 ± 1.2ab	68.0 ± 1.1ab	17.2 ± 0.4b	25.0 ± 0.5c	61.40 ± 2.3f
Bw	21.5 ± 0.5 b	0.60 ± 0.02a	12.2 ± 0.3c	0.7 ± 0.1b	2.8 ± 0.2d	0.6 ± 0.1a	1.5 ± 0.1c	82.2 ± 1.3bc	68.0 ± 1.1ab	16.5 ± 0.4a	25.4 ± 0.5c	33.50 ± 1.3a
Bc0.1%	22.0 ± 0.5 bc	0.60 ± 0.02a	11.9 ± 0.3b	0.6 ± 0.1a	2.4 ± 0.2ab	1.5 ± 0.1b	1.3 ± 0.1b	82.3 ± 1.3c	69.0 ± 1.2bc	17.5 ± 0.4b	24.8±0.5 bc	43.42 ± 1.6c
Bc0.2%	21.0 ± 0.5 ab	0.62 ± 0.02b	12.1 ± 0.3bc	0.8 ± 0.1c	2.7 ± 0.2cd	2.1 ± 0.2d	1.5 ± 0.1c	80.8 ± 1.2ab	66.5 ± 1.0a	17.0 ± 0.4ab	25.2 ± 0.5c	39.40 ± 1.5b
Bc0.3%	22.0 ± 0.5 bc	0.61 ± 0.02a b	12.4 ± 0.3c	0.7 ± 0.1b	2.6 ± 0.2bc	2.7 ± 0.2e	1.2 ± 0.1a	80.4 ± 1.2a	68.2 ± 1.1ab	18.1 ± 0.5c	25.7 ± 0.6c	42.60 ±1.6b c
Bk0.1%	22.2 ± 0.5 bc	0.63 ± 0.02b	11.7 ± 0.3a	0.5 ± 0.1a	2.5 ± 0.2ab c	0.9 ± 0.1a	1.4 ± 0.1bc	83.0 ± 1.4d	70.1 ± 1.3d	17.6 ± 0.4b	24.9±0.5 bc	38.50 ± 1.4b
Bk0.2%	21.8 ± 0.5 bc	0.58 ± 0.02a	12.6 ± 0.3d	0.9 ± 0.1d	2.4 ± 0.2ab	1.5 ± 0.1b	1.3 ± 0.1b	81.3 ± 1.2ab	67.9 ± 1.0a	19.0 ± 0.6d	26.2 ± 0.6d	50.70 ± 1.9d
Bk0.3%	22.0	0.65	11.4 ±	0.6 ±	2.3 ±	2.1 ±	1.1 ±	82.5 ±	70.5 ±	17.5	24.6±0.5	63.63

	± 0.5 bc	± 0.02c	0.3a	0.1a	0.2a	0.2d	0.1a	1.3c	1.3d	± 0.4b	bc	± 2.4e
Cw	22.5 ± 0.5 c	0.62 ± 0.02b	12.1 ± 0.3c	0.7 ± 0.1b	2.4 ± 0.2a	0.6 ± 0.1a	1.3 ± 0.1b	82.9 ± 1.4d	70.0 ± 1.3d	18.9 ± 0.5d	25.0 ± 0.5b	31.05 ± 1.2a
Cc0.1%	22.0 ± 0.5 bc	0.62 ± 0.02b	12.0 ± 0.3bc	0.8 ± 0.1c	2.5 ± 0.2ab	1.5 ± 0.1b	1.4 ± 0.1c	81.8 ± 1.3c	69.5 ± 1.2cd	18.0 ± 0.4c	24.7 ± 0.5b	51.15 ± 1.9d
Cc0.2%	22.2 ± 0.5 bc	0.59 ± 0.02a	11.6 ± 0.3a	0.5 ± 0.1a	2.2 ± 0.2a	1.8 ± 0.1c	1.2 ± 0.1a	82.7 ± 1.4d	70.8 ± 1.4d	19.0 ± 0.6d	25.1 ± 0.5b	55.37 ± 2.1e
Cc0.3%	22.5 ± 0.5 c	0.63 ± 0.02c	12.3 ± 0.3d	0.7 ± 0.1b	2.6 ± 0.2b	2.4 ± 0.2d	1.3 ± 0.1b	80.7 ± 1.2b	68.3 ± 1.1b	21.5 ± 0.7e	25.8 ± 0.6c	46.41 ± 1.7c
Ck0.1%	22.0 ± 0.5 bc	0.61 ± 0.02a b	11.8 ± 0.3ab	0.6 ± 0.1a	2.4 ± 0.2a	1.2 ± 0.1a	1.1 ± 0.1a	82.9 ± 1.4d	69.2 ± 1.2c	18.6 ± 0.5cd	24.8 ± 0.5b	50.37 ± 1.9d
Ck0.2%	22.5 ± 0.5 c	0.64 ± 0.02c	12.5 ± 0.3d	0.9 ± 0.1d	2.7 ± 0.2b	1.5 ± 0.1b	1.5 ± 0.1c	80.9 ± 1.2b	66.7 ± 1.0a	20.3 ± 0.6e	25.5±0.5 bc	52.67 ±2.0d e
Ck0.3%	23.0 ± 0.5 c	0.60 ± 0.02a	11.9 ± 0.3ab	0.8 ± 0.1c	2.5 ± 0.2ab	2.1 ± 0.2c	1.4 ± 0.1bc	81.3 ± 1.2bc	68.8 ± 1.1bc	19.2 ± 0.6d	24.9 ± 0.5b	63.23 ± 2.4f

A=12.2% unhydrated (direct mill), B=hydrated 15%, C= hydrated 16%, w = water extraction, k=base extraction, c=acid extraction.

3.2. Hydration and treatment reactions

Increasing hydration from 12.2% to 16% improved yield only when combined with sodium hydroxide (Ak0.3%: 61.40% → Ck0.3%: 63.23%), while acetate treatments showed effects independent of hydration (Bc0.1%: 43.42% → Cc0.1%: 51.15%). The reduction in particle size (0.58–0.65 μm) is more pronounced in the high-yield sodium hydroxide treatments (Bk0.3%: 0.65 μmc), indicating improved starch granule isolation. Moisture content (11.4–13%) and ash content (0.5–0.9%) remained stable across samples, confirming that the treatment effects outweighed the wetting effects and that the resulting aggregates conformed to the functional properties. The highest levels (f) consistently showed optimal starch purity (≥ 68%), moderate amylose (17–21%), and low fiber content (≤ 2.5%).

Table 3 Functional properties of starch isolated from millet flour.

Sample	Bulk Density (g/cm³)	Water Absorption (g/g)	Oil Absorption (g/g)
AW (12.2%)	20.5 ± 0.4 a	1.50 ± 0.05 a	1.00 ± 0.04 ab
AC0.1%	21.5 ± 0.5 b	1.70 ± 0.06 b	1.05 ± 0.04 b
AC0.2%	22.5 ± 0.5 c	1.90 ± 0.07 c	1.10 ± 0.05 b
AC0.3%	20.0 ± 0.4 a	1.45 ± 0.05 a	0.95 ± 0.04 a
Ak0.1%	20.8 ± 0.5 ab	1.55 ± 0.05 ab	0.92 ± 0.04 a
Ak0.2%	21.0 ± 0.5 ab	1.60 ± 0.06 ab	0.90 ± 0.04 a
Ak0.3%	20.5 ± 0.5 a	1.40 ± 0.05 a	0.93 ± 0.04 a
BW (15%)	21.5 ± 0.5 b	1.50 ± 0.06 a	0.91 ± 0.04 a
BC0.1%	22.0 ± 0.5 bc	1.55 ± 0.06 ab	0.90 ± 0.04 a
BC0.2%	21.0 ± 0.5 ab	1.65 ± 0.05 b	1.00 ± 0.04 ab
BC0.3%	22.0 ± 0.5 bc	1.75 ± 0.06 bc	0.98 ± 0.04 ab
BK0.1%	22.2 ± 0.5 bc	1.80 ± 0.06 bc	0.95 ± 0.04 a
BK0.2%	21.8 ± 0.5 bc	1.65 ± 0.05 b	1.00 ± 0.04 ab
BK0.3%	22.0 ± 0.5 bc	1.70 ± 0.06 b	0.97 ± 0.04 ab
CW (16%)	22.5 ± 0.5 c	1.75 ± 0.06 bc	0.95 ± 0.04 a
Cc0.1%	22.0 ± 0.5 bc	1.85 ± 0.06 c	1.05 ± 0.04 b
Cc0.2%	22.2 ± 0.5 bc	1.88 ± 0.06 c	1.02 ± 0.04 ab
Cc0.3%	22.5 ± 0.5 c	1.90 ± 0.07 c	1.00 ± 0.04 ab
Ck0.1%	22.0 ± 0.5 bc	1.80 ± 0.06 bc	1.00 ± 0.04 ab
Ck0.2%	22.5 ± 0.5 c	1.85 ± 0.06 c	0.98 ± 0.04 ab
Ck0.3%	23.0 ± 0.5 c	1.90 ± 0.07 c	0.95 ± 0.04 a

* Values with the same superscript letter within a column are not significantly different ($p > 0.05$).

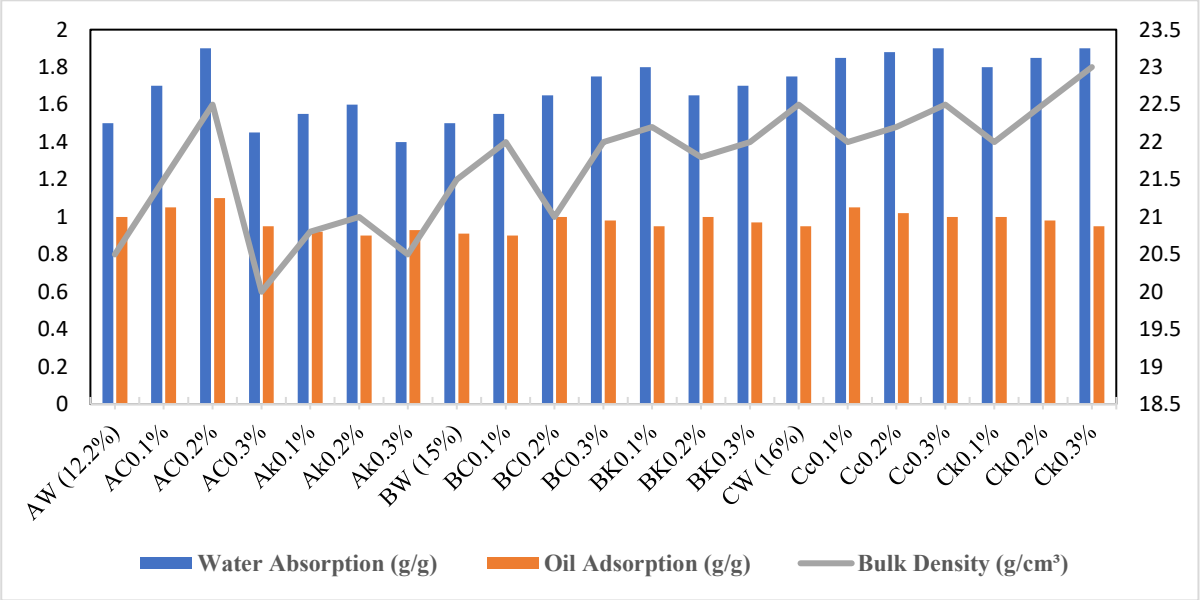

Figure 1 Functional properties of starch extracted (aqueous, acidic, basic) from millet flour at different moisture contents.

The apparent density, water absorption capacity (WAC), and oil adsorption capacity (OAC) of the extracted millet starches are strongly affected by both hydration level and extraction method. Apparent density values are divided into three statistical groups (c–a), with the highest density observed for CK 0.3% (23 g/cm³) at 16% hydration. This indicates that a higher concentration of sodium hydroxide enhances starch granule compaction and packing efficiency. In general, increasing the hydration rate of millet flour from 12.2% to 16% led to denser starches, particularly in samples extracted using sodium hydroxide and sodium acetate. A similar trend is noted for aqueously extracted starches (Aw, Bw, and Cw), where apparent density increased progressively from 20.5 to 22.5 g/cm³ with higher hydration levels. Water absorption capacity also showed clear differentiation into three statistical groups (c–a). The highest WAC values (1.8–1.9 g/g) are recorded for sodium hydroxide- and sodium acetate-extracted starches, especially at 16% hydration, reflecting enhanced water-binding ability resulting from chemical modification and greater exposure of hydrophilic sites. Samples with moderate hydration effects exhibited lower WAC values ranging from 1.40 to 1.65 g/g. Oil adsorption capacity formed two statistical groups (a and b), with the highest OAC observed in acetate-treated starch at 12.2% hydration (AC 0.2%: 1.10 g/g). However, OAC decreased with increasing hydration, reaching 0.95 g/g at 16% hydration. Higher sodium hydroxide concentration further reduced oil adsorption, demonstrating that hydration level and chemical treatment jointly alter starch surface properties [46-50].

Table 4 Solubility (%) of millet starch at different temperatures with statistical groupings.

Sample	55°C	65°C	75°C	85°C	95°C
AW	8.5 ± 0.3a	14.0 ± 0.5a	20.5 ± 0.7a	28.0 ± 0.9a	37.0 ± 1.2a
AC0.1%	10.0 ± 0.4b	15.5 ± 0.6b	22.0 ± 0.8b	30.0 ± 1.0b	40.0 ± 1.3b
AC0.2%	9.5 ± 0.3ab	14.8 ± 0.5ab	21.5 ± 0.7ab	29.5 ± 1.0ab	39.0 ± 1.3ab
AC0.3%	10.2 ± 0.4b	16.0 ± 0.6b	23.0 ± 0.8bc	31.0 ± 1.0bc	41.5 ± 1.4bc
Ak0.1%	11.0 ± 0.4c	17.0 ± 0.6c	24.0 ± 0.8cd	32.5 ± 1.1cd	42.0 ± 1.4cd
Ak0.2%	9.8 ± 0.3b	15.2 ± 0.5b	22.5 ± 0.8b	30.5 ± 1.0b	38.5 ± 1.3ab
Ak0.3%	10.5 ± 0.4bc	16.5 ± 0.6bc	23.5 ± 0.8c	31.5 ± 1.1c	43.0 ± 1.4d
BW	10.0 ± 0.4b	15.6 ± 0.6b	22.1 ± 0.8b	30.3 ± 1.0b	40.2 ± 1.3b
BC0.1%	10.8 ± 0.4c	16.2 ± 0.6bc	23.8 ± 0.8cd	32.0 ± 1.1cd	40.5 ± 1.4bc
BC0.2%	9.0 ± 0.3a	15.0 ± 0.5ab	21.0 ± 0.7a	29.0 ± 1.0a	38.0 ± 1.3a
BC0.3%	10.1 ± 0.4b	15.8 ± 0.6b	22.2 ± 0.8b	30.8 ± 1.0b	41.0 ± 1.4bc
BK0.1%	11.5 ± 0.4d	17.5 ± 0.6d	24.5 ± 0.8d	33.0 ± 1.1d	44.0 ± 1.5e
BK0.2%	9.7 ± 0.3b	15.3 ± 0.5b	21.7 ± 0.7ab	29.7 ± 1.0ab	39.5 ± 1.3ab
BK0.3%	10.3 ± 0.4b	16.1 ± 0.6b	23.2 ± 0.8bc	31.2 ± 1.0bc	42.5 ± 1.4de
CW	11.2 ± 0.4cd	17.2 ± 0.6cd	24.2 ± 0.8cd	32.8 ± 1.1d	43.8 ± 1.5e
Cc0.1%	9.2 ± 0.3a	14.5 ± 0.5a	21.2 ± 0.7a	28.5 ± 1.0a	36.5 ± 1.2a
Cc0.2%	10.6 ± 0.4bc	16.4 ± 0.6bc	23.6 ± 0.8cd	31.8 ± 1.1cd	43.5 ± 1.5e
Cc0.3%	8.8 ± 0.3a	14.3 ± 0.5a	20.8 ± 0.7a	27.8 ± 0.9a	36.0 ± 1.2a
Ck0.1%	10.7 ± 0.4bc	16.6 ± 0.6cd	23.9 ± 0.8cd	32.2 ± 1.1cd	41.8 ± 1.4cd
Ck0.2%	9.6 ± 0.3b	15.4 ± 0.5b	21.6 ± 0.7ab	29.6 ± 1.0ab	39.2 ± 1.3ab
Ck0.3%	10.4 ± 0.4b	16.3 ± 0.6bc	23.4 ± 0.8bc	31.4 ± 1.0bc	42.0 ± 1.4cd

*Values with the same superscript letter within a column are not significantly different ($p>0.05$).

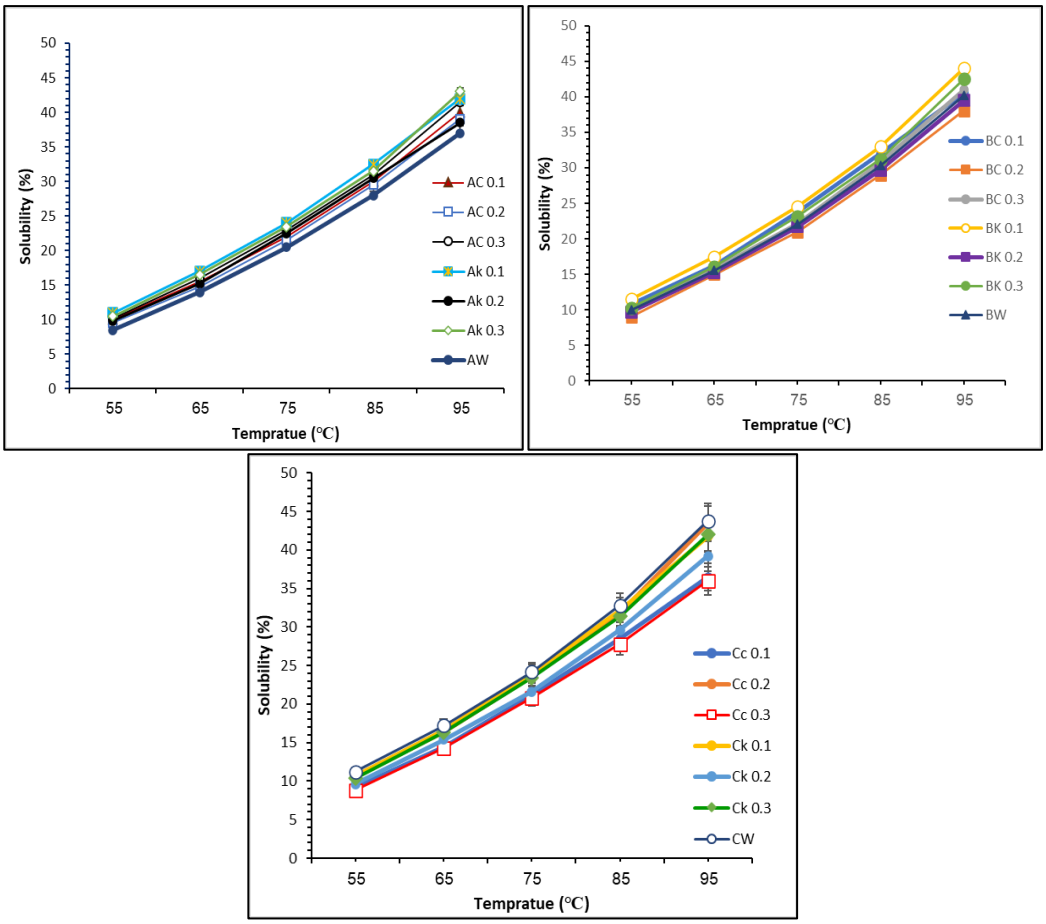

Figure 2 Solubility of starch extracted from millet flour at different temperatures.

Starch solubility showed a strong dependence on temperature, chemical treatment, and hydration level. Solubility increased progressively with rising temperature, ranging from 8.5–11.5% at 55 °C to 36.0–44.0% at 95 °C, with four to five distinct statistical groups observed at each temperature. At 95 °C, samples separated into five groups (a–e), where alkaline and aqueous extractions consistently exhibited the highest solubility values, notably BK 0.1% (44.0%) and CW (43.8%). For aqueously extracted starches (AW, BW, and CW), solubility is clearly moisture-dependent, increasing with hydration level and reaching a maximum at 16% hydration. Chemical treatment significantly influenced dissolution behavior across all temperatures. Sodium hydroxide treatments consistently formed statistically superior groups compared to acetate-treated starches. At 75 °C, alkaline-extracted starches (23.4–24.5%) outperformed acetate samples (20.8–23.6%). A concentration of 0.1% proved optimal for both chemicals, with BK 0.1% achieving the highest solubility across all tested temperatures (11.5–44%). Acetate treatments displayed concentration-dependent effects; at 95 °C, AC 0.3% showed higher solubility than AC 0.1%, whereas Cc 0.3% performed slightly worse than Cc 0.1%. Hydration level interacted strongly with chemical treatment. Higher hydration (16%) enhanced solubility in sodium hydroxide–treated starches but reduced solubility in acetate-treated samples. The most pronounced hydration effect is observed in aqueous starch, where increased hydration markedly improved solubility at high temperature, highlighting the dominant plasticizing role of water in unmodified starch systems [51-55].

Table 5 Swelling Power (g/g) of millet starch at different temperatures with statistical groupings.

Sample	55°C	65°C	75°C	85°C	95°C
AW	7.0 ± 0.3a	8.5 ± 0.4a	11.0 ± 0.5a	14.0 ± 0.6a	16.5 ± 0.7a
AC0.1%	8.0 ± 0.3bc	9.5 ± 0.4bc	12.0 ± 0.5bc	15.0 ± 0.6bc	18.0 ± 0.7bc
AC0.2%	7.5 ± 0.3ab	9.0 ± 0.4ab	11.5 ± 0.5ab	14.5 ± 0.6ab	17.0 ± 0.7ab
AC0.3%	8.2 ± 0.3cd	9.7 ± 0.4cd	12.5 ± 0.5cd	15.5 ± 0.6cd	18.5 ± 0.7cd
Ak0.1%	8.5 ± 0.3de	10.0 ± 0.4de	13.0 ± 0.5de	16.0 ± 0.6de	19.0 ± 0.7de
Ak0.2%	7.8 ± 0.3bc	9.3 ± 0.4bc	12.2 ± 0.5bc	15.2 ± 0.6bc	17.5 ± 0.7bc
Ak0.3%	8.3 ± 0.3cd	9.8 ± 0.4cd	12.8 ± 0.5cd	15.8 ± 0.6cd	19.2 ± 0.7de
BW	8.0 ± 0.3bc	9.4 ± 0.4bc	12.6 ± 0.5cd	15.6 ± 0.6cd	18.1 ± 0.7cd
BC0.1%	8.6 ± 0.3e	10.2 ± 0.4e	13.2 ± 0.5e	16.2 ± 0.6e	19.2 ± 0.7de
BC0.2%	7.7 ± 0.3ab	9.1 ± 0.4ab	11.7 ± 0.5ab	14.2 ± 0.6ab	17.3 ± 0.7ab
BC0.3%	8.1 ± 0.3cd	9.6 ± 0.4cd	12.3 ± 0.5cd	15.3 ± 0.6cd	18.2 ± 0.7cd
BK0.1%	8.7 ± 0.3e	10.3 ± 0.4e	13.5 ± 0.5e	16.5 ± 0.6e	19.5 ± 0.7e
BK0.2%	7.6 ± 0.3ab	9.2 ± 0.4ab	12.0 ± 0.5bc	14.0 ± 0.6a	17.2 ± 0.7ab
BK0.3%	8.4 ± 0.3de	10.1 ± 0.4de	13.1 ± 0.5de	16.1 ± 0.6de	19.1 ± 0.7de
CW	8.9 ± 0.3f	10.5 ± 0.4f	13.6 ± 0.5f	16.6 ± 0.6f	19.6 ± 0.7e
Cc0.1%	7.9 ± 0.3bc	9.0 ± 0.4ab	11.8 ± 0.5ab	14.3 ± 0.6ab	17.4 ± 0.7ab
Cc0.2%	8.5 ± 0.3de	10.0 ± 0.4de	13.0 ± 0.5de	16.0 ± 0.6de	19.0 ± 0.7de
Cc0.3%	6.9 ± 0.3g	8.4 ± 0.4g	10.9 ± 0.5g	13.9 ± 0.6g	16.2 ± 0.7g
Ck0.1%	8.8 ± 0.3f	10.4 ± 0.4f	13.4 ± 0.5ef	16.4 ± 0.6ef	19.4 ± 0.7e
Ck0.2%	7.4 ± 0.3h	9.1 ± 0.4ab	11.6 ± 0.5ab	14.1 ± 0.6ab	17.1 ± 0.7ab
Ck0.3%	8.2 ± 0.3cd	9.9 ± 0.4cd	12.7 ± 0.5cd	15.7 ± 0.6cd	18.3 ± 0.7cd

*Values with the same superscript letter within a column are not significantly different ($p>0.05$).

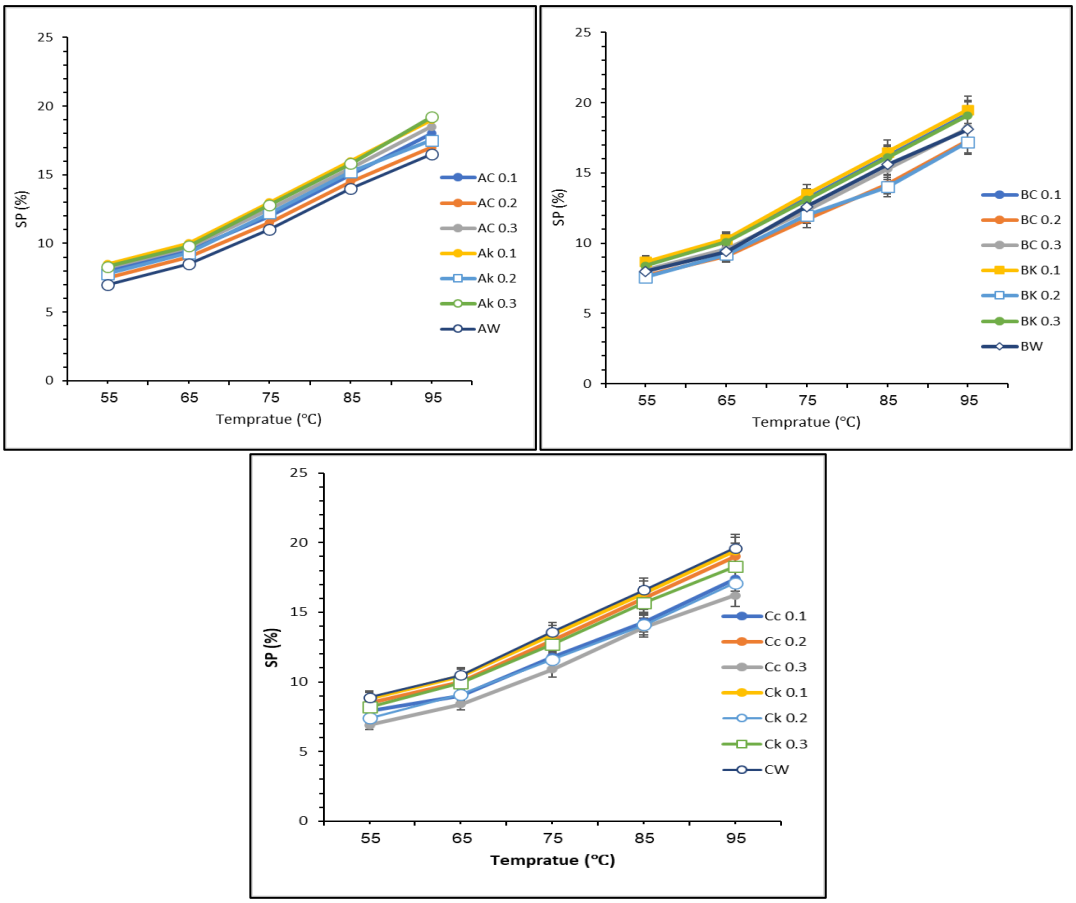

Figure 3 The swelling power of starch extracted from millet flour at different temperatures.

Swelling power of millet starch increased progressively with temperature, rising from 6.9–8.9 g/g at 55 °C to 16.2–19.6 g/g at 95 °C, with six to seven statistical clusters observed at each temperature. At 95 °C, the samples are separated into five distinct groups (g–a), where sodium hydroxide and aqueous extraction methods consistently exhibited the highest swelling intensity, notably BK 0.1% (19.5 g/g) and CW (19.6 g/g) [56-60]. For aqueously extracted starches (AW, BW, and CW), swelling is strongly dependent on hydration level, with 16% hydration (CW) producing the maximum swelling intensity [61-65]. Chemical treatment significantly influenced swelling behavior across all temperatures. Sodium hydroxide treatments consistently formed statistically superior clusters compared with acetate-treated starches [66-70]. At 75 °C, alkaline-extracted starches showed higher swelling (13.1–13.6 g/g) than acetate samples (10.9–12.5 g/g). A concentration of 0.1% is optimal for both chemicals, with BK 0.1% achieving peak swelling across the entire temperature range (8.7–19.5 g/g) [71-75]. Acetate treatments exhibited concentration-dependent responses; at 95 °C, AC 0.3% displayed greater swelling than AC 0.1%, whereas Cc 0.3% showed reduced swelling compared to Cc 0.1%. Hydration level interacted strongly with chemical treatment [76, 77]. Higher hydration (16%) enhanced swelling in sodium hydroxide–treated starches but reduced swelling in acetate-treated samples. The most pronounced hydration effect is observed in hydro-extracted starch, where increased moisture led to a substantial rise in swelling at high temperature, highlighting the dominant role of hydration in unmodified starch systems [78-80].

3.3. Effect of nanotechnology on starch properties

The incorporation of nanotechnology into starch processing significantly enhances its physicochemical and functional properties. Nanoscale modification leads to reduced particle size, increased surface area, and improved water absorption capacity [81-85]. These changes result in enhanced solubility, swelling power, and interaction with other components [86]. Furthermore, nano-assisted extraction techniques improve starch purity and functional performance, making the material more suitable for advanced food and industrial applications [87]. Table 6 presents a comparative evaluation of conventional and nano-modified starch, demonstrating significant enhancement in functional and physicochemical properties due to nanoscale modification [88].

Table 6 Comparison between conventional starch and nanotechnology-modified starch highlighting improvements in particle size, water absorption, solubility, and swelling properties.

Parameter	Conventional Starch	Nano-Modified Starch
Particle Size	Micron scale	Nanoscale
Water Absorption	Moderate	High
Solubility	Moderate	Enhanced
Swelling Power	Moderate	High
Surface Area	Limited	Increased

Figure 4 presents the impact of nanotechnology on starch functionality, highlighting enhanced physicochemical behavior and improved performance compared to conventional starch.

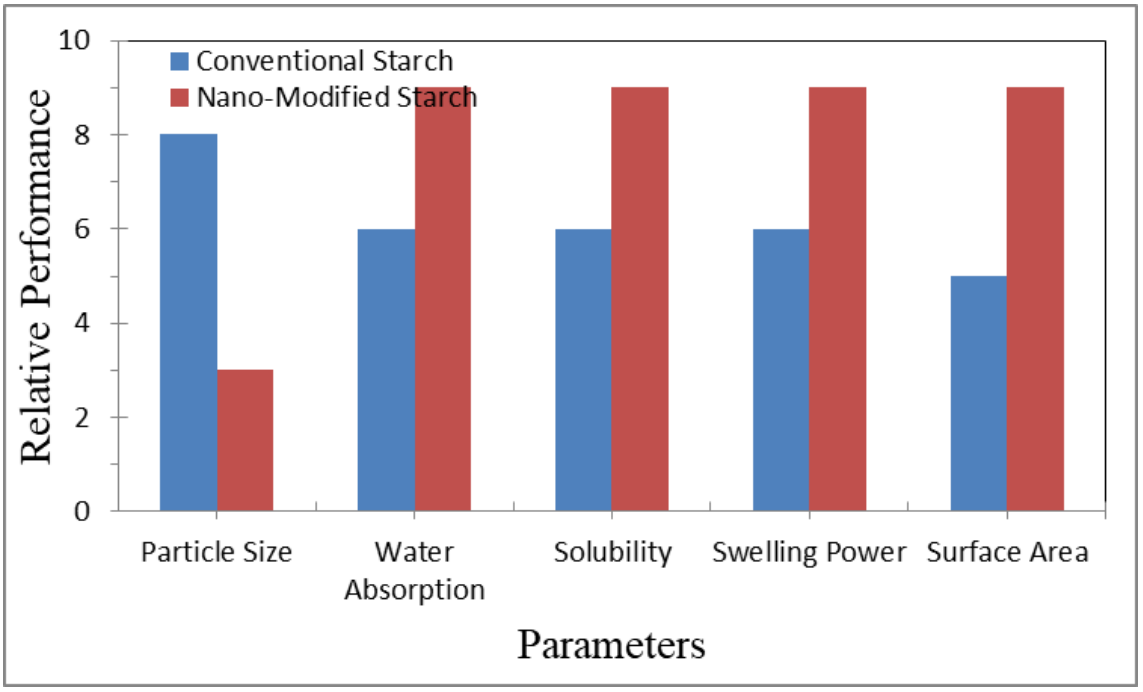

Figure 4 Effect of nanotechnology on starch properties showing improvements in particle size reduction and functional performance.

4. CONCLUSIONS

The extraction conditions played a decisive role in determining the quality and functional behavior of foxtail millet starch beyond yield alone. Alkaline extraction proved particularly effective in improving starch recovery and modifying granule characteristics, producing finer particles with enhanced water absorption and functional performance. Acid treatment, while reducing amylose content, promoted higher protein association at increased concentrations, indicating partial disruption of starch–protein interactions. Hydration rate was also a critical factor, as higher grain hydration generally enhanced starch density and functional properties, especially under chemical extraction conditions. Differences observed in solubility, swelling power, and oil adsorption capacity suggest that each extraction method imparts distinct structural modifications to starch granules. Overall, the results demonstrate that careful selection of hydration level and extraction medium can tailor millet starch properties for specific food and industrial applications, supporting its potential as a versatile alternative starch source in product formulation and processing. The integration of nanotechnology into starch extraction and processing offers a powerful approach to enhancing functional and physicochemical properties of millet starch. Nanoscale modification improves particle size distribution, increases surface area, and enhances hydration behavior, leading to superior performance in food and industrial applications. Future research should focus on applying nano-assisted techniques to further optimize starch functionality and expand its potential applications.

References

[1] T.E. Friedemann, N.F. Witt, *J. AOAC Int.* 50 (1967) 958. https://doi.org/10.1093/jaoac/50.4.958.
[2] G.K. Adkins, C.T. Greenwood, Carbohydr. Res. 3 (1966) 81. https://doi.org/10.1016/S0008-6215(00)82299-5.
[3] M. McCleary, B.V. McCleary, collaborative study, *J. AOAC Int.* 80 (1997) 571. https://doi.org/10.1093/jaoac/80.3.571.
[4] P.J. Van Soest, J.B. Robertson, B.A. Lewis, *J. Dairy Sci.* 74 (1991) 3583. https://doi.org/10.3168/jds.S0022-0302(91)78551-2.
[5] H. Atrous, N. Benbettaieb, M. Chouaibi, H. Attia, D. Ghorbel, Int. J. Food Prop. 20 (2017) 1532. https://doi.org/10.1080/10942912.2016.1216211.
[6] J. Jane, *J. Appl. Glycosci.* 53 (2006) 205. https://doi.org/10.5458/jag.53.205.
[7] U.D. Chavan et al., J. Food Sci. Technol. 53 (2016) 1. https://doi.org/10.1007/s13197-015-2050-8.
[8] M. Eshel, M. Levy, U. Mingelgrin, U. Singer, *Soil Sci. Soc. Am. J.* 68 (2004) 736. https://doi.org/10.2136/sssaj2004.0736.
[9] M.Z. Dar et al., Int. J. Biol. Macromol. 108 (2018) 1348. https://doi.org/10.1016/j.ijbiomac.2017.11.119.
[10] H.O. Egharevba, IntechOpen (2019). https://doi.org/10.5772/intechopen.86629.
[11] J. Gao, T. Vasanthan, R. Hoover, Cereal Chem. 86 (2009) 157. https://doi.org/10.1094/CCHEM-86-2-0157.
[12] T.S. Gibson, V.A. Solah, B.V. McCleary, A, J. Cereal Sci. 25 (1996) 111. https://doi.org/10.1006/jcrs.1996.0021.
[13] Heena et al., Heliyon 10 (2024) e25330. https://doi.org/10.1016/j.heliyon.2024.e25330
[14] R. Hoover et al., Food Chem. 56 (1996) 355. https://doi.org/10.1016/0308-8146(95)00194-8.
[15] J.R.N. Taylor, A. Taylor, *Food Sci. Technol. Int.* 22 (2016) 1. https://doi.org/10.1177/1082013215582245.
[16] K.S. Sandhu et al., Carbohydr. Polym. (2021) 100073. https://doi.org/10.1016/j.carpta.2021.100073.

[17] O. Calvin, Afr. J. Food Sci. 10 (2016) 344. https://doi.org/10.5897/AJFS2016.1481
[18] P. Mahajan et al., Int. J. Biol. Macromol. 180 (2021) 61. https://doi.org/10.1016/j.ijbiomac.2021.03.063.
[19] A.J. Palacios-Fonseca et al., J. Food Eng. 93 (2009) 45. https://doi.org/10.1016/j.jfoodeng.2009.01.006.
[20] S. Park, Y.R. Kim, Clean label starch: Food Sci. Biotechnol. 30 (2020) 1. https://doi.org/10.1007/s10068-020-00834-3
[21] S.P. Bangar et al., Carbohydr. Polym. (2022) 119265. https://doi.org/10.1016/j.carbpol.2022.119265.
[22] S.P. Bangar et al., Int. J. Biol. Macromol. 190 (2021) 960. https://doi.org/10.1016/j.ijbiomac.2021.09.064
[23] S. Singh et al., J. Agric. Food Chem. 58 (2010) 1180. https://doi.org/10.1021/jf903770j.
[24] S. Punia et al., Carbohydr. Polym. 260 (2021) 117776. https://doi.org/10.1016/j.carbpol.2021.117776.
[25] S. Srichuwong, J.I. Jane, Food Sci. Biotechnol. 16 (2007) 663.
[26] L. Wang, Y.J. Wang, Cereal Chem. 78 (2001) 690. https://doi.org/10.1094/CCHEM.2001.78.6.690.
[27] Y. Ai, J.L. Jane, Starch/Stärke 67 (2015) 213. https://doi.org/10.1002/star.201400201
[28] Y. Yang et al., Food Chem. 331 (2020) 127315. https://doi.org/10.1016/j.foodchem.2020.127315.
[29] Y. Zhao et al., J. Funct. Foods 6 (2014) 499. https://doi.org/10.1016/j.jff.2013.11.012.
[30] A. A. Hateef, E. Dhahri, M. Rasheed, H. Kadhim, Z. Abbas, N. Hassan, Physics and Chemistry of Solid State, 25 (2024) 801. https://doi.org/10.15330/pcss.25.4.801-810.
[31] A. Boumezoued, K. Guergouri, Régis Barillé, Rechem Djamil, Mourad Zaabat, M. Rasheed, J. Alloys Compd. 791 (2019) 550. https://doi.org/10.1016/j.jallcom.2019.03.251.
[32] A. I. A. Ali, M. RASHEED, Experimental and Theoretical NANOTECHNOLOGY, 10 (2026) 277. https://doi.org/10.56053/10.s.277.
[33] A. I. A. Ali, M. RASHEED, Experimental and Theoretical NANOTECHNOLOGY, 10 (2026) 239. https://doi.org/10.56053/10.s.239.
[34] A. Jaber, M. Ismael, T. Rashid, M. A. Sarhan, M. Rasheed, I. M. Sala. Eureka: Phys. Eng. 4 (2023) 29. https://doi.org/10.21303/2461-4262.2023.002770
[35] A. Keziz, M. Heraiz, F. Sahnoune, M. Rasheed, Ceram. Int. 49 (2023) 32989. https://doi.org/10.1016/j.ceramint.2023.07.275
[36] A. Keziz, M. Heraiz, M. RASHEED, A. Oueslati. Mater Chem. Phys. 325 (2024) 129757. https://doi.org/10.1016/j.matchemphys.2024.129757
[37] A. Khaleefah, M. RASHEED, Experimental and Theoretical NANOTECHNOLOGY, 10 (2026) 289. https://doi.org/10.56053/10.s.289.
[38] A. R. J. Katae, H. H. Hussein, A. S. Jaber, M. A. Sarhan, M. RASHEED, Experimental and Theoretical NANOTECHNOLOGY, 10 (2026) 357. https://doi.org/10.56053/10.s.357.
[39] A. R. J. Katae, H. H. Hussein, A. S. Jaber, M. A. Sarhan, M. RASHEED, Experimental and Theoretical NANOTECHNOLOGY, 10 (2026) 795. https://doi.org/10.56053/10.2.795.
[40] F. Boudou, et al., Not. Sci. Biol. 17 (2025) 12593. https://doi.org/10.55779/nsb17312593
[41] F. Dkhilalli, S. M. Borchani, M. Rasheed, R. Barille, K. Guidara, M. Megdiche, J. Mater. Sci. Mater. Electron, 29 (2018) 6297. https://doi.org/10.1007/s10854-018-8609-z.
[42] H. K. Aity, E. Dhahri, M. Rasheed. Ceram. Int. 50 (2024) part B 54666. https://doi.org/10.1016/j.ceramint.2024.10.324
[43] H. K. Aity, M. Rasheed, E. Dhahri, A. A. Hateef, T. Saidani, Journal of Materials Science, 61 (2026) 6226. https://doi.org/10.1007/s10853-026-12241-w.
[44] I. Alshalal, H. M. I. Al-Zuhairi, A. A. Abtan, M. Rasheed, M. K. Asmail. J. Mech. Behav. Mater. 32 (2023) 1. https://doi.org/10.1515/jmbm-2022-0280

[45] I.M. Mohammed, M. Rasheed, AIP Conf. Proc. 3321 (2025) 020026. https://doi.org/10.1063/5.0289719
[46] M. A. Sarhan, S. Shihab, B. E. Kashem, M. Rasheed, J. Phy.: Conf. Ser., 1879 (2021) 022122. https://doi.org/10.1088/1742-6596/1879/2/022122.
[47] M. Enneffatia, M. Rasheed, B. Louati, K. Guidara, S. Shihab, R. Barillé, J. Phys.: Conf. Ser. 1795 (2021) 012050. https://doi.org/10.1088/1742-6596/1795/1/012050
[48] M. M. Najim, B. A. Yousif, M. RASHEED, Experimental and Theoretical NANOTECHNOLOGY, 10 (2026) 551. https://doi.org/10.56053/10.2.551.
[49] M. M. Najim, B. A. Yousif, M. RASHEED, Experimental and Theoretical NANOTECHNOLOGY, 10 (2026) 627. https://doi.org/10.56053/10.2.627
[50] M. Rasheed et al., J. Phys.: Conf. Ser. 1999 (2021) 012080. https://doi.org/10.1088/1742-6596/1999/1/012080
[51] M. RASHEED, A. Khaleefah, Materials Chemistry and Physics, 353 (2026) 132112. https://doi.org/10.1016/j.matchemphys.2026.132112.
[52] M. Rasheed, et al., J. Adv. Biotechnol. Exp. Ther. 6 (2023) 495. https://doi.org/10.5455/jabet.2023.d144
[53] M. Rasheed, I. Alshalal, A.A. Ashed, M.A. Sarhan, A.S. Jaber, Indones. J. Electr. Eng. Comput. Sci. 33 (2024) 653. https://doi.org/10.11591/ijeecs.v33.i1.pp653-660
[54] M. Rasheed, M. N. Mohammedali, F. A. Sadiq, M. A. Sarhan, T. Saidani. J. Optics (New Delhi. Print) 54 (2024) 3490. https://doi.org/10.1007/s12596-024-01928-5
[55] M. Rasheed, M. Nuhad Al-Darraji, S. Shihab, A. Rashid, T. Rashid. J. Phys.: Conf. Ser. 1963 (2021) 012058. https://doi.org/10.1088/1742-6596/1963/1/012058
[56] M. Rasheed, M.N. Al-Darraji, S. Shihab, A. Rashid, T. Rashid, J. Phys.: Conf. Ser. 1963 (2021) 012059. https://doi.org/10.1088/1742-6596/1963/1/012059
[57] M. Rasheed, O. Alabdali, S. Shihab, A. Rashid, T. Rashid, J. Phys.: Conf. Ser. 1999 (2021) 012078. https://doi.org/10.1088/1742-6596/1999/1/012078
[58] M. Rasheed, O. Alabdali, S. Shihab, J. Phy.: Conf. Ser. 1879 (2021) 032120. https://doi.org/10.1088/1742-6596/1879/3/032120.
[59] M. Rasheed, O.Y. Mohammed, S. Shihab, A. Al-Adili, J. Phys.: Conf. Ser. 1795 (2021) 012043. https://doi.org/10.1088/1742-6596/1795/1/012043
[60] M. Rasheed, R. Barillé, J. Non-Cryst. Solids., 476 (2017) 1. https://doi.org/10.1016/j.jnoncrysol.2017.04.027.
[61] M. Rasheed, R. Barillé, Opt. Quantum Electron. 49 (2017). https://doi.org/10.1007/s11082-017-1030-7.
[62] M. Rasheed, S. Shihab, O. Alabdali, A. Rashid, T. Rashid, J. Phys.: Conf. Ser. 1999 (2021) 012077. https://doi.org/10.1088/1742-6596/1999/1/012077
[63] M. Rasheed, SuhaShihab, O. Alabdali, H. H. Hassan, J. Phys. Conf. Ser., 1879 (2021) 032113. https://doi.org/10.1088/1742-6596/1879/3/032113
[64] M. Sellam, M. Rasheed, S. Azizi, T. Saidani. Ceram. Int. 50 (2024) 20917. https://doi.org/10.1016/j.ceramint.2024.03.094
[65] N. Assoudi et al. Opt. Quant. Electron. 54 (2022) 9. https://doi.org/10.1007/s11082-022-03927-x
[66] N. Ben Azaza et al., Opt. Mater., 96 (2019) 109328. https://doi.org/10.1016/j.optmat.2019.109328.
[67] O. Alabdali, S. Shihab, M. Rasheed, T. Rashid. 3rd inter. Scient. conf. alkafeel univ. (ISCKU 2021) 2386 (2022) 050019. https://doi.org/10.1063/5.0066860
[68] R. Jalal, S. Shihab, M.A. Alhadi, M. Rasheed, J. Phys.: Conf. Ser. 1660 (2020) 012090. https://doi.org/10.1088/1742-6596/1660/1/012090
[69] R.S. Mahmood et al. J. Mech. Behav. Mater. 34 (2025) 1. https://doi.org/10.1515/jmbm-2025-0040

[70] S. S. Batros, M. Rasheed, H. K. Aity, A. A. Hatef, T. Saidani, Materials Chemistry and Physics, 355 (2026) 132243. https://doi.org/10.1016/j.matchemphys.2026.132243.
[71] S. Shihab, M. Rasheed, O. Alabdali, A.A. Abdulrahman, J. Phys.: Conf. Ser. 1879 (2021) 022120. https://doi.org/10.1088/1742-6596/1879/2/022120
[72] T. Rashid, M. M. Mokji, M. Rasheed. J. Optics 54 (2024) 3490. https://doi.org/10.1007/s12596-024-02080-w
[73] T. Rashid, M.M. Mokji, M. Rasheed, J. Mech. Behav. Mater. 34 (2025) 77. https://doi.org/10.1515/jmbm-2025-0074
[74] T. Saidani, M. Rasheed, I. Alshalal, A.A. Rashed, M.A. Sarhan, R. Barillé, Res. Eng. Struct. Mater. 10 (2024) 743. http://dx.doi.org/10.17515/resm2023.21ma0922rs
[75] T. Saidani, S. Mokhtari, M. Rasheed, H. Lahmar, M. Trari, Journal of the Indian Chemical Society, 103 (2026) 102499. https://doi.org/10.1016/j.jics.2026.102499.
[76] Z. S. Ahmed, M. RASHEED, H. S. Ahmed, Experimental and Theoretical NANOTECHNOLOGY, 10 (2026) 329. https://doi.org/10.56053/10.s.329.
[77] Z. S. Ahmed, M. RASHEED, H. S. Ahmed, Experimental and Theoretical NANOTECHNOLOGY, 10 (2026) 343. https://doi.org/10.56053/10.s.343.
[78] A. Raghdi, M. Heraiz, M. Rasheed, A. Keziz, Journal of the Indian Chemical Society, 101 (2024) 101413. https://doi.org/10.1016/j.jics.2024.101413.
[79] A. Zubaidi, L.M. Asaad, I. Alshalal, M. Rasheed, J. Mech. Behav. Mater. 32 (2023) 1. https://doi.org/10.1515/jmbm-2022-0302
[80] A.H. Ali, A.S. Jaber, M.T. Yaseen, M. Rasheed, O. Bazighifan, T.A. Nofal, Complexity 2022 (2022) 1. https://doi.org/10.1155/2022/9367638
[81] A.J. Hussein, M.N. Al-Darraji, M. Rasheed, M.A. Sarhan, IOP Conf. Ser.: Earth Environ. Sci. 1262 (2023) 022007. https://doi.org/ 10.1088/1755-1315/1262/2/022007
[82] A.J. Hussein, M.N. Al-Darraji, M. Rasheed, M.A. Sarhan, IOP Conf. Ser.: Earth Environ. Sci. 1262 (2023) 022005. https://doi.org/10.1088/1755-1315/1262/2/022005
[83] D. Bouras, M. Rasheed, Opt. Quantum Electron. 54 (2022) 12. https://doi.org/10.1007/s11082-022-04161-1
[84] D. Kherifi, A. Keziz, M. Rasheed, A. Oueslati. Ceram. Int. 50 part A (2024) 30175. https://doi.org/10.1016/j.ceramint.2024.05.317
[85] E. Arif, R. Jamal, M. RASHEED, Experimental and Theoretical NANOTECHNOLOGY, 10 (2026) 453. https://doi.org/10.56053/10.2.453
[86] E. Kadri, K. Dhahri, R. Barillé, M. Rasheed. Phase Transi. 94 (2021) 65. https://doi.org/10.1080/01411594.2020.1832224
[87] F. Boudou, A. Belakredar, A. Berkane, M. Rasheed. Not. Sci. Biol. 17 (2025) 12183. https://doi.org/10.55779/nsb17212183
[88] F. Boudou, A. Guendouzi, A. Belkredar. M. Rasheed, Not. Sci. Biol. 16 (2024) 13837. https://doi.org/10.55779/nsb16211837